Neutron depolarization by antiferromagnetic particles

R. Rosman and M. Th. Rekveldt
Interfacultair Reactor Instituut, Delft University of Technology, 2629 JB Delft, The Netherlands
(Received 25 February 1991)

Neutron-depolarization theory in ensembles of antiferromagnetic particles is discussed by using the scattering approach. The magnetic inhomogeneities in the ensembles are the ferromagnetic planes of the particles. These may result in depolarization in principle in two ways. In the first place it occurs by Bragg scattering; however, as the Bragg angles generally exceed the aperture of the analyzer, Bragg scattering may contribute to the depolarization in exceptional cases only. Secondly, possible planes at the surface of the particles, the mean magnetization of which is not compensated by that of a neighboring plane, scatter at small angles; therefore such "uncompensated" planes can contribute to the depolarization. The theory is compared to the results of neutron-depolarization measurements on compacts of α-Fe_2O_3 and Cr particles.

I. INTRODUCTION

The three-dimensional neutron-depolarization (ND) technique is a powerful method to study static and dynamic properties of magnetic structures in the micrometer and submicrometer region (e.g., Refs.1–8). In a ND experiment, the polarization vector of a polarized neutron beam is analyzed after transmission through a magnetic medium. During transmission, the polarization vector is affected by magnetic inhomogeneities in the medium: mean magnetic induction results in a net rotation of the polarization vector around the former, while variations in the local magnetic induction result in an effective shortening of the polarization vector, called depolarization henceforth. A ND experiment yields the magnetic correlation length along the neutron path of variations in the local magnetization, the mean orientation of these variations (magnetic texture) and the mean magnetization, in general. The range of magnetic correlation lengths which can be measured covers 10 nm up to mm's, making ND, to some extent, complementary to small-angle neutron scattering (SANS).

Recently, neutron depolarization by compacts of (antiferromagnetic) α-Fe_2O_3 (hematite) particles has been observed.[8] Additional measurements on compacts of Cr (chromium) particles yielded a surprisingly large correlation parameter ξ which appeared to be dependent on the neutron wavelength and the aperture of the analyzer used. In this paper, ND by antiferromagnetic particles is discussed.

In ND theory, two types of approaches exist: the *Larmor* and the *scattering* approach.[9,10] The former approach is based on the Larmor precession of the polarization vector of a polarized neutron beam around magnetic inhomogeneities. It neglects the broadening of the neutron beam as a result of scattering. The scattering approach is based on small-angle scattering by magnetic inhomogeneities and obviously takes the broadening of the neutron beam into account. As this broadening is essential in the interpretation of ND measurements on antiferromagnetic particles, the scattering approach is used in this paper.

Section II deals with the theory of ND in ensembles of antiferromagnetic particles. Section III gives the results of ND measurements on compacts of α-Fe_2O_3 and Cr particles. These results are discussed in Sec. IV. Section V contains the main conclusions.

Although neutron-diffraction experiments on antiferromagnets have been performed for many years (one of the first neutron-diffraction experiments on α-Fe_2O_3 is described in Ref. 11), ND by antiferromagnets was not treated before.

II. THEORY OF ND IN ANTIFERROMAGNETIC PARTICLES

According to the scattering approach, a ND experiment on an ensemble of magnetic particles with a mean magnetization equal to zero yields a correlation matrix $\hat{\alpha}$, the components α_{ij} $(i,j=x,y,z)$ of which are given by[9]

$$\alpha_{ij}=\frac{8\pi^4}{\langle V\rangle}\int\langle B_i(\boldsymbol{\kappa})B_j(-\boldsymbol{\kappa})\rangle d^2\boldsymbol{\kappa} \tag{1}$$

with

$$\mathbf{B}(\boldsymbol{\kappa})=\frac{\mu_0}{(2\pi)^3}\int_V \mathbf{M}^*(\mathbf{r},\tilde{\boldsymbol{\kappa}})e^{i\boldsymbol{\kappa}\cdot\mathbf{r}}d^3\mathbf{r}\ , \tag{2}$$

$$\mathbf{M}^*(\mathbf{r},\tilde{\boldsymbol{\kappa}})=\tilde{\boldsymbol{\kappa}}\times[\mathbf{M}(\mathbf{r})\times\tilde{\boldsymbol{\kappa}}]\ . \tag{3}$$

Here, V is the particle volume, $\langle\ \rangle$ an average over all particles, $\boldsymbol{\kappa}$ the scattering vector, and $\tilde{\boldsymbol{\kappa}}=\boldsymbol{\kappa}/|\boldsymbol{\kappa}|$. The quantity $\mathbf{B}(\boldsymbol{\kappa})$ is equivalent to the structure factor used in scattering theory. The integration over $\boldsymbol{\kappa}$ is over those scattering vectors which correspond to scattering angles τ smaller than the aperture of the analyzer. The scattering vector is related to the scattering angle by

$$\kappa=\frac{4\pi}{\lambda}\sin(\tau/2) \tag{4}$$

with λ the neutron wavelength.

This section deals with the depolarization by an ensemble of magnetically uncorrelated isotropically distributed antiferromagnetic particles. For such an ensemble, $\hat{\alpha}$ is

diagonal and the quantities

$$\xi=\sum_i \alpha_{ii} \ , \tag{5}$$

$$\gamma_i=\alpha_{ii}/\xi \tag{6}$$

are used instead of α_{ij}. Roughly speaking, the correlation parameter ξ is the product of $[\mu_0 M(\mathbf{r})]^2$ and the correlation length of $M^2(\mathbf{r})$ along the propagation direction $\mathbf{e}_0$ of the neutron beam. The quantities γ_i approximate the mean values of n_i^2, with $\mathbf{n}$ the unit vector along $\mathbf{M}(\mathbf{r})$. For an ensemble of isotropically distributed ferromagnetic particles with $\mathbf{e}_0$ along $\mathbf{z}$,[9]

$$\gamma_x=\tfrac{1}{4} \ , \quad \gamma_y=\tfrac{1}{4} \ , \quad \gamma_z=\tfrac{1}{2} \ . \tag{7}$$

An antiferromagnet has a mean magnetization equal to zero and is therefore commonly not considered to be a magnetic inhomogeneity. However, the ferromagnetic planes within the antiferromagnet represent magnetic inhomogeneities which result in scattering. Due to the antiparallel orientation of the magnetization in two neighboring planes, the depolarization by these two planes, referred to as a *unit cell* is small. The term "unit cell" used in this paper should not be confused with the corresponding term commonly used in solid-state physics.

Two types of scattering processes may exist. In the first place, the periodicity of the unit cell results in Bragg scattering. Obviously only those scattered neutrons that enter the analyzer contribute to the depolarization. This depolarization, which results in a correlation parameter ξ independent of the particle size, is discussed in Sec. II A. Secondly, due to the irregular shape of the particles, some ferromagnetic planes at the surface of the particle may exist which do not form part of a unit cell and hence scatter independently. The depolarization by these planes, which is discussed in Sec. II B, depends on the particle shape. The larger the particle, the smaller the relative contribution of such *uncompensated planes.* The details of the calculations involved are given in Appendixes A and B.

Bragg scattering by ferromagnetic planes also occurs in ferromagnetic media. However, as will be shown in Sec. II A, it contributes to the depolarization in exceptional cases only because the scattering angles involved are generally much in excess of the aperture of the analyzer. Furthermore, even if the aperture of the analyzer would be large so that Bragg scattering occurs within the analyzer, the corresponding depolarization effect is negligibly small in comparison to the depolarization by the ferromagnetic domain structure.

A. Depolarization due to Bragg scattering

The depolarization by an ensemble of isotropically distributed rectangular antiferromagnetic particles with size $2A$, $2B$, and $2C$ along X, Y, and Z is considered. Each particle contains $2N$ ferromagnetic planes with size a along X ($A=Na$, $a \ll A,B,C$), which are parallel to the YZ plane (note that a real antiferromagnetic particle has many types of ferromagnetic planes). As already mentioned, two neighboring planes will be referred to as a unit cell. Figure 1 (Appendix A) gives one particle out of the ensemble.

Due to the periodicity of the unit cell in the X direction, scattering only occurs at

$$\kappa \approx k\pi/a \tag{8}$$

with k an integer. Equation (8) expresses the Bragg law. It follows from the value of $\mathbf{B}(\boldsymbol{\kappa})$ for a unit cell (see Appendix A) that most of the scattering occurs for $k=1$ ($\kappa \approx \pi/a$). The reason that no scattering occurs at $\kappa=0$ is that the mean magnetization of the particles equals zero.

The aperture of the analyzer of a ND instrument, τ_m, is small (typically 0.01–0.1 rad), which has the following consequences. In the first place, only Bragg scattering by ferromagnetic planes with

$$a > \frac{\lambda}{2\tau_m} \tag{9}$$

occurs within the aperture of the analyzer. Hence, only these planes may contribute to the depolarization. Secondly, since the scattering angles should be small, only Bragg scattering by planes which are about parallel to the propagation direction of the neutron beam may occur within the aperture of the analyzer.

It can be shown (Appendix A) that the Bragg scattering by ferromagnetic planes which satisfy Eq. (9) results in a contribution to ξ equal to

$$\xi=0.27(\mu_0 M)^2 a \ . \tag{10}$$

The quantities γ_i appear to be given by Eq. (7) (see Appendix A).

Since an antiferromagnetic particle contains different kind of ferromagnetic planes, the correlation parameter ξ of the ensemble is given by

$$\xi=0.27\sum_k (\mu_0 M_k)^2 a_k \ . \tag{11}$$

Here the sum is over all those planes which satisfy Eq. (9).

B. Depolarization due to uncompensated planes

Antiferromagnetic particles may contain ferromagnetic planes at the surface which do not belong to a unit cell. These uncompensated planes act as magnetic inhomogeneities and result in scattering and therewith in depolarization.

The depolarization by a single plane with sizes a, $2E$, and $2F$ along X, Y, and Z is considered. An example of a plane is given in Fig. 3 of Appendix B. The local magnetization $\mathbf{M}$ is again in the YZ plane. As the mean magnetization of the plane differs from zero, the scattering occurs around $\kappa=0$. Assuming $E=F$, most of the scattering occurs at scattering vectors in the range (see Appendix B)

$$0 \le \kappa < 2\pi/E \ . \tag{12}$$

Therefore, when

$$E > \frac{\lambda}{\tau_m} , \tag{13}$$

most of the scattered neutrons enter the analyzer and contribute to the depolarization.

The correlation parameter ξ of a single plane depends on a, E, and F and exceeds a. Figure 4 of Appendix B gives $\xi/[a(\mu_0 M)^2]$ vs p when $E=F=pa$. The correlation length ξ exceeds a and increases with increasing p. Obviously, the value of ξ will be somewhat smaller than according to Fig. 4 when part of the scattering occurs outside the aperture of the analyzer. It is calculated in Appendix B that γ_i obeys Eq. (7).

As the quantities γ_i of both an ensemble of uncorrelated ferromagnetic planes (see above) as well as an ensemble of rectangular antiferromagnetic particles (see Sec. II A) are given by Eq. (7), the values of γ_i for an ensemble of antiferromagnetic particles containing uncompensated planes are the same. The correlation parameter ξ of the latter ensemble is given by

$$\xi=(1-r)\xi_1+r\xi_2 . \tag{14}$$

Here r is the fractional size of the uncompensated planes of the particle, ξ_1 the value of ξ given by Eq. (11), and ξ_2 the value of ξ given in Fig. 4 of Appendix B. When the particle volume increases, r, and therewith the contribution of ξ_2 to ξ, decreases.

III. EXPERIMENTAL RESULTS

The hematite compact used in the ND experiments was supplied by BASF.[12] The particles are monocrystalline common antiferromagnets with a rhombohedral structure. Their shape is acicular with a mean diameter of 40 nm and an aspect ratio of 8. At room temperature, α-Fe_2O_3 has a local magnetization of 1630 kA/m and possesses a weak ferromagnetic component of 0.9 kA/m.

The Cr particles (99.98% Cr) are purchased from Ventron,[13] have a mean size in the order of 100 μm, and are polycrystalline. The local magnetization of Cr (bcc structure) is complex. Neutron-diffraction measurements revealed an in first approximation simple antiferromagnetic structure (see Refs. 14–19). Superimposed on this simple anti-ferromagnetic structure, a long-range incommensurate spin-density wave exists with a period of about 25 unit cells at room temperature. The maximum of the local magnetization is 390 kA/m (room temperature). Extensive reviews about chromium are given in Refs. 20 and 21.

The ND experiments have been performed on two different instruments, *KP* and *SP*. Instrument *KP* has Cu_2MnAl crystals magnetized to saturation as a polarizer and analyzer and uses neutrons with a wavelength $\lambda=0.16\pm0.01$ nm (the polarizer simultaneously acts as a monochromator). The aperture of the analyzer is around 0.02 rad. Instrument *SP* has Co-Fe mirrors magnetized to saturation as a polarizer and analyzer and a pyrolythic graphite crystal in Bragg reflection as a monochromator ($\lambda=0.35\pm0.03$ nm). The aperture of its analyzer is 0.1 rad along the x direction and 0.01 rad along the y direction. Both instruments use coils as polarization turners.

The parameters ξ and γ_i of the α-Fe_2O_3 and the Cr compact have been determined on both *KP* and *SP*. The depolarization by the α-Fe_2O_3 was too small to determine ξ accurately on *KP* (the depolarization effect on *KP* is smaller due to the smaller neutron wavelength). The quantities γ_i of the α-Fe_2O_3 compact could not be determined on either instrument. The results of the measurements are summarized in Table I. The parameter ϵ in this table is the particle volume fraction. The quantity ξ_B for α-Fe_2O_3 is the expected value for ξ based on the Bragg scattering by the (111) planes of α-Fe_2O_3 ($M=1630$ kA/m and $a=0.230$ nm). The real contribution of the Bragg scattering to ξ will be somewhat larger than the value of ξ_B as more planes contribute to the depolarization. It appears that the observed value of ξ of the α-Fe_2O_3 compact is about half ξ_B.

The value of the correlation parameter ξ of the Cr compact as determined on *KP* is about three times the value determined using *SP*. Both values of ξ of the Cr are surprisingly large and much in excess of the value of ξ_B, which is based on Bragg scattering by the (100), the (010), and the (001) planes ($M=390$ kA/m and $a=0.288$ nm have been used). Furthermore, the correlation parameter ξ in Cr highly exceeds that in α-Fe_2O_3. The values of γ_i determined in the Cr compact differ from those given by Eq. (7).

IV. DISCUSSION

In α-Fe_2O_3, the ferromagnetic planes with the largest spacing are the (111) planes, corresponding to $a=0.230$ nm. According to Eq. (4), the Bragg scattering by these planes occurs mainly at $\tau=0.35$ rad on *KP* and at $\tau=0.78$ rad on *SP*. Bragg scattering by the other planes occurs at even larger scattering angles, so that Bragg scattering only occurs well beyond the aperture of the analyzer. Consequently, no depolarization related to Bragg scattering is expected to be observed [ξ_1 in Eq. (14)

TABLE I. The parameters ξ and γ_i of the α-Fe_2O_3 and Cr compacts. The aperture of the analyzer of *KP* is around 0.02 rad, that of *SP* 0.1 rad in the x direction and 0.01 rad in the y direction.

Compact	Instrument	ξ (nm T^2)	γ_x (±0.03)	γ_y (±0.03)	γ_z (±0.03)	ϵ	ξ_B (nm T^2)
α-Fe_2O_3	*SP*	0.15 ± 0.05				0.23	0.3
α-Fe_2O_3	*KP*	<0.4				0.23	0.3
Cr	*SP*	0.6 ± 0.1	0.31	0.32	0.37	0.52	0.06
Cr	*KP*	1.6 ± 0.2	0.32	0.30	0.38	0.52	0.06

equals zero] and the observed depolarization is likely to be mainly due to the scattering by the uncompensated planes as discussed in Sec. II B. If they represent only a few volume percent of the particles, these planes may already account for the observed depolarization. As an example, values for ξ_2 and r of Eq. (14) of $3a(\mu_0 M)^2$ (corresponding to $p=20$ in Fig. 4) and 0.05, respectively, already yield the value of ξ observed in α-Fe_2O_3.

Possibilities other than the uncompensated planes, which may account for the observed depolarization in α-Fe_2O_3, are depolarization related to multiple scattering and to the weak ferromagnetic component. The contribution of the latter to ξ is calculated to be about 2×10^{-5} nm T^2, a contribution which is much smaller than the value of ξ observed. Also the depolarization due to multiple scattering is negligibly small.

The observation that the value of ξ for the Cr compact determined on *KP* is about three times that determined on *SP* indicates that part of the scattering which is measured on *KP* occurs outside the aperture of the analyzer of *SP*. However, also on *KP*, part of the scattering occurs outside the analyzer, following from the observed values of γ_i which differ from those given by Eq. (7). The observation that the value of γ_z in Cr determined on both instruments is smaller than $\frac{1}{2}$ indicates that, in particular when the local magnetization is along $\mathbf{e}_0$, not all scattered neutrons enter the analyzer.

Bragg scattering by the simple antiferromagnetic structure cannot account for the observed depolarization in Cr for different reasons. All Bragg scattering by this structure occurs outside the analyzers of the ND instruments. This can easily be seen from the smallest scattering angle. This angle, which is the scattering angle related to the (001) planes ($a=0.288$ nm), is $\tau=0.28$ rad on *KP* and $\tau=0.62$ rad on *SP*. Moreover, the theoretical contribution of the Bragg scattering to the correlation parameter, i.e., 0.06 nm T^2, is much smaller than the values of ξ observed in Cr. Furthermore, the observed values of γ_i differ from those expected for depolarization related to Bragg scattering [see Eq. (7)].

Also, uncompensated planes at the surface of the Cr crystallites cannot account for the observed depolarization in the Cr compact, since the contribution of these planes is much smaller than the values of ξ observed. Consequently, the observed depolarization in Cr can be related neither to Bragg scattering by the simple antiferromagnetic structure nor to small-angle scattering by uncompensated planes.

Another possibility, which, in principle, may account for the observed values of ξ in the Cr compact, is Bragg scattering by the spin-density wave. This scattering will occur around $\tau=0.02$ rad at instrument *KP* and around $\tau=0.05$ rad at *SP*. The former scattering angle equals the aperture of the analyzer of *KP*, as a result of which Bragg scattering by the spin-density wave may contribute to the depolarization. The calculated scattering angle for *SP* exceeds the aperture of the analyzer in the y direction and is smaller than the aperture in the x direction, implying that only a small fraction of the scattered neutrons may result in depolarization. However, as a result of the simple antiferromagnetic structure in Cr, the scattering amplitude of the spin-density wave and hence the contribution to ξ of the spin-density wave is extremely low.

Note that, if the Cr particles are oxidized at the surface, this ferromagnetic layer is expected to contribute to the depolarization. However, the volume fraction of the surface layer is so low that this contribution is negligible.

In summary, the observed depolarization in Cr, interpreted in terms of the ND theory formulated in Sec. II, cannot be explained using the local magnetic structure of Cr reported in the literature. The origin of the large value for the correlation parameter, a value which indicates the presence of magnetic inhomogeneities larger than those possible according to the known structure of Cr, is not understood

V. SUMMARY AND CONCLUSIONS

ND theory in ensembles of antiferromagnetic particles has been discussed. It has been shown that generally Bragg scattering does not contribute to the depolarization since the scattering angles involved well exceed the aperture of the analyzer. Scattering by possible uncompensated planes at the surface of the particles, the mean magnetization of which is not compensated by that of a neighboring plane, occurs at small angles. Consequently, such planes contribute to the depolarization. The theory is applied to the results of ND measurements on compacts of α-Fe_2O_3 and Cr particles. The depolarization observed in the α-Fe_2O_3 compact is such that it can be attributed to uncompensated planes. The observed neutron depolarization in the Cr compact cannot be explained with a simple antiferromagnetic structure on which a spin-density wave is superimposed.

ACKNOWLEDGMENTS

The authors express their thanks to Professor J. J. van Loef for a critical reading of the manuscript.

APPENDIX A: THE DEPOLARIZATION BY AN ENSEMBLE OF RECTANGULAR ANTIFERROMAGNETIC PARTICLES

The correlation parameter ξ and the quantities γ_i of an ensemble of isotropically distributed antiferromagnetic particles as described in Sec. II A is considered. In order to simplify the calculations involved, it is assumed that one of the axes of the x,y,z and the X,Y,Z systems always coincide. This assumption only slightly affects the calculations made. Furthermore, it is assumed that the angle between the local magnetization and the Z axis is ϕ.

In the calculations the following procedure will be followed. At first, the depolarization matrix by an individual particle, denoted $\hat{\beta}$, is considered. It is assumed that the Y axis of the particle and the y axis of the system coincide while the angle between the x and X axes and between the z and Z axes is θ (Fig. 1). This depolarization matrix is related to the X,Y,Z system of the particle. Thereafter, the diagonal elements α_{ii} of the ensemble, which is related to the x,y,z system, are derived using

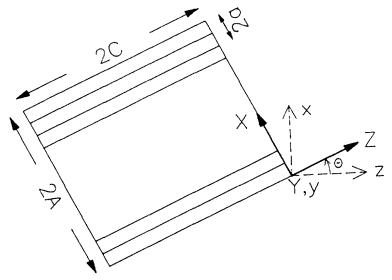

FIG. 1. A sketch of a rectangular antiferromagnetic particle.

$$\alpha_{xx}=\alpha_{yy}=(\langle\bar{\beta}_{XX}\cos^2\theta\rangle+\langle\bar{\beta}_{ZZ}\sin^2\theta\rangle+\langle\bar{\beta}_{YY}\rangle)/2\ ,$$
$$\alpha_{zz}=\langle\bar{\beta}_{XX}\sin^2\theta\rangle+\langle\bar{\beta}_{ZZ}\cos^2\theta\rangle\ . \tag{A1}$$

Here $\langle\ \rangle$ means an average over θ and the overbar means an average over ϕ. Finally, the correlation parameter ξ and the quantities γ_i can be calculated from α_{ii} using Eqs. (5) and (6). At first it will be assumed that scattering occurs at small angles so that all scattered neutrons enter the analyzer.

As $\kappa_z=0$, with $\boldsymbol{\kappa}$ the scattering vector in the xyz system, the scattering vectors in the xyz and in the XYZ systems, the latter denoted **s**, are related by

$$\mathbf{s}_X=\kappa_x\cos\theta\ ,$$
$$\mathbf{s}_Y=\kappa_y\ , \tag{A2}$$
$$\mathbf{s}_Z=\kappa_x\sin\theta\ .$$

It can be calculated from Eqs. (1)–(3) that the correlation matrix of a ferromagnetic particle as given in Fig. 1 is given by

$$\beta_{II}(\theta)=\frac{\pi^4}{aBC}\int f_I(\boldsymbol{\kappa},\theta,\phi)g(\boldsymbol{\kappa},\theta)d^2\kappa\ . \tag{A3}$$

The function

$$f_I(\boldsymbol{\kappa},\theta,\phi)=B_I'(\boldsymbol{\kappa},\theta,\phi)B_I'(-\boldsymbol{\kappa},\theta,\phi) \tag{A4}$$

describes the scattering of the unit cell. The quantity $\mathbf{B}'(\boldsymbol{\kappa},\theta,\phi)$ is the value of $\mathbf{B}(\boldsymbol{\kappa})$ for the unit cell and follows from

$$B_X'(\boldsymbol{\kappa},\theta,\phi)=-(\tilde{\kappa}_x\tilde{\kappa}_y\cos\theta\sin\phi+\tilde{\kappa}_x^2\cos\phi\sin\theta\cos\theta)h(\boldsymbol{\kappa},\theta)\ ,$$
$$B_Y'(\boldsymbol{\kappa},\theta,\phi)=(\tilde{\kappa}_x^2\sin\phi-\tilde{\kappa}_x\tilde{\kappa}_y\sin\theta\cos\phi)h(\boldsymbol{\kappa},\theta)\ , \tag{A5}$$
$$B_Z'(\boldsymbol{\kappa},\theta,\phi)=[(1-\tilde{\kappa}_x^2\sin^2\theta)\cos\phi-\tilde{\kappa}_x\tilde{\kappa}_y\sin\phi\sin\theta]h(\boldsymbol{\kappa},\theta)\ ,$$

with

$$h(\boldsymbol{\kappa},\theta)=\mu_0 M\frac{aBC}{\pi^3}\left[\frac{\sin(\kappa_x C\sin\theta)}{\kappa_x C\sin\theta}\frac{\sin(\kappa_y B)}{\kappa_y B}\times\frac{\sin^2[(\kappa_x a\cos\theta)/2]}{(\kappa_x a\cos\theta)/2}\right]. \tag{A6}$$

The function $g(\boldsymbol{\kappa},\theta)$ describes the effect of the periodicity of the unit cell in the X direction and is given by

$$g(\boldsymbol{\kappa},\theta)\approx\frac{\pi}{a}\sum_{k=-\infty}^{\infty}\delta\left[\kappa_x-k\frac{\pi}{a\cos\theta}\right]. \tag{A7}$$

Scattering only occurs around $\boldsymbol{\kappa}$ vectors with $\kappa_x=(k\pi)/(a\cos\theta)$.

Figure 2 gives the functions $h_1(x)=[(\sin x)/x]^2$ and $h_2(x)=[(\sin^2 x/x]^2$ for $x\geq 0$. The functions h_1 and h_2 differ substantially from zero only for $0\leq x<\pi$ and $0<x<\pi$, respectively, with h_1 maximum at $x=0$ and h_2 maximum at $x=0.37\pi$. Scattering only occurs when both $h(\boldsymbol{\kappa},\theta)$ and $g(\boldsymbol{\kappa},\theta)$ differ from zero. Following from Fig. 2, Eqs. (A6) and Eq. (A7), the latter is the case only when

$$0\leq\kappa_y<\pi/B \tag{A8}$$

and

$$k_x\approx k\pi/(a\cos\theta)\ , \tag{A9}$$
$$0\leq\kappa_x<\pi/(C\sin\theta)\ , \tag{A10}$$
$$0<\kappa_x<2\pi/(a\cos\theta)\ . \tag{A11}$$

It follows that scattering only occurs at $\theta\ll 1$ and furthermore that $\kappa_x\approx\pi/a$ and $\kappa_y\approx 0$. As a result, the amplitude of the scattering vector is around π/a. The reason that no scattering occurs at $\kappa=0$ is because the mean magnetization of the particle equals zero.

It follows from Eqs. (A4)–(A6) that, for $\theta^2\ll 1$,

$$f_I(\boldsymbol{\kappa},\theta,\phi)=(\delta_{IY}\sin^2\phi+\delta_{IZ}\cos^2\phi)[h'(\boldsymbol{\kappa},\theta)]^2 \tag{A12}$$

with δ_{IJ} the Kronecker δ and $h'(\boldsymbol{\kappa},\theta)$ the value of $h(\boldsymbol{\kappa},\theta)$ given by Eq. (A6) in which $\cos\theta$ is approximated by 1. In the calculation of Eq. (A12) it has been assumed that, for those $\boldsymbol{\kappa}$ vectors that contribute to β_{II}, $\tilde{\kappa}_x\approx 1$, and $\tilde{\kappa}_y\approx 0$. The validity of the latter assumption follows from the fact that those $|\kappa_y|$ values which most contribute to β_{II} are smaller than π/Y while those $|\kappa_x|$ values which most contribute to β_{II} are about π/a with $a\ll Y$.

It follows from Eqs. (A3), (A7), and (A12) and from

$$\int_{-\infty}^{\infty}\left[\frac{\sin(\kappa_y B)}{\kappa_y B}\right]^2 d\kappa_y=\pi/B \tag{A13}$$

that

$$\bar{\beta}_{II}(\theta)=\tfrac{1}{2}(\delta_{IY}+\delta_{IZ})j(\theta) \tag{A14}$$

with

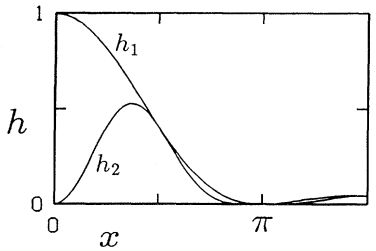

FIG. 2. The functions $h_1(x)$ and $h_2(x)$.

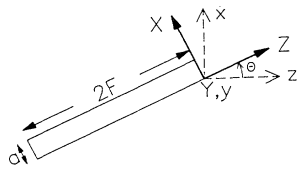

FIG. 3. A sketch of a single ferromagnetic plane.

$$j(\theta)=\frac{8C(\mu_0M)^2}{\pi^2}\times\sum_{k=0}^{\infty}\left[\frac{\sin[(2k+1)(\sin\theta)\pi C/a]}{(2k+1)^2(\sin\theta)\pi C/a}\right]^2 . \quad \text{(A15)}$$

In Eq. (A15), the integration over κ_x has been replaced by a summation over k with $\kappa_x=(2k+1)\pi/a$. It follows from Eqs. (5), (A1), (A14), and (A15) that the correlation parameter ξ of the total ensemble is given by

$$\xi=\frac{2}{\pi}\int_0^{\pi/2}j(\theta)d\theta \quad \text{(A16)}$$

$$\approx\frac{8a(\mu_0M)^2}{\pi^3}\sum_{k=0}^{\infty}\frac{1}{(2k+1)^3} \quad \text{(A17)}$$

$$\approx 0.27a(\mu_0M)^2 \quad \text{(A18)}$$

independent of A, B, or C. The values of γ_i approximate to those given by Eq. (7). Small deviations from the values given by Eq. (7) are due to the assumption that one of the axes of the x,y,z and the X,Y,Z systems always coincide. In the derivation of Eq. (A17) from Eq. (A16), the assumption $\theta^2 \ll 1$ has been used again.

It is stressed that, in the above, it has been assumed that all scattered neutrons enter the analyzer. This is only the case as long as

$$a > \frac{\lambda}{2\tau_m} \quad \text{(A19)}$$

with τ_m the aperture of the analyzer.

APPENDIX B: THE DEPOLARIZATION BY AN ENSEMBLE OF FERROMAGNETIC PLANES

The correlation parameter ξ and the quantities γ_i of an ensemble of isotropically distributed ferromagnetic planes as described in Sec. II B is considered. The same procedure as used in Appendix A will be followed. The angle between the local magnetization in the plane and the Z axis is again denoted ϕ. Furthermore, it is assumed that the Y axis of the plane coincides with the y axis of the system and the angle between the x and X axes and between the z and Z axes is denoted θ (Fig. 3).

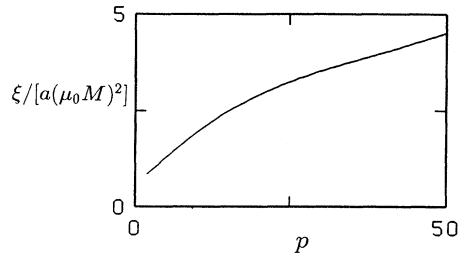

FIG. 4. The quantity $\xi/[a(\mu_0M)^2]$ of an ensemble of isotropically distributed ferromagnetic planes vs p.

Following from Eqs. (1)–(3) and (A2), the diagonal elements β_{II} of the correlation matrix of the single ferromagnetic plane given in Fig. 3 averaged over ϕ are given by

$$\begin{aligned}\overline{\beta_{XX}(\theta)}&=\tilde{\kappa}_x^2\cos^2\theta(\tilde{\kappa}_y^2+\tilde{\kappa}_x^2\sin^2\theta)o(\boldsymbol{\kappa},\theta)\ ,\\ \overline{\beta_{YY}(\theta)}&=\tilde{\kappa}_x^2(\tilde{\kappa}_x^2+\tilde{\kappa}_y^2\sin^2\theta)o(\kappa,\theta)\ ,\\ \overline{\beta_{ZZ}(\theta)}&=[1-\tilde{\kappa}_x^2\sin^2\theta(2-\tilde{\kappa}_y^2-\tilde{\kappa}_x^2\sin^2\theta)]o(\boldsymbol{\kappa},\theta)\ ,\end{aligned} \quad \text{(B1)}$$

with

$$o(\boldsymbol{\kappa},\theta)=\frac{(\mu_0M)^2}{2\pi^2}aDE\times\int d\kappa_x\int d\kappa_y\left[\frac{\sin(\kappa_x a\cos\theta)}{\kappa_x a\cos\theta}\frac{\sin(\kappa_y D)}{\kappa_y D}\times\frac{\sin(\kappa_x E\sin\theta)}{\kappa_x E\sin\theta}\right]^2 . \quad \text{(B2)}$$

For $\theta=0$ ($\tilde{\kappa}_x\approx 0$),

$$\bar{\beta}_{II}\approx\tfrac{1}{2}(\delta_{IY}+\delta_{IZ})E\ . \quad \text{(B3)}$$

Under the assumption $D=E=pa$, ξ and γ_i have been numerically calculated from Eqs. (5), (6), (A1), and (B1) for several values of p. It appeared that the quantities γ_i are given by Eq. (7), independent of p. The quantity ξ increases with increasing p (Fig. 4).

It follows from Eq. (B2) that most of the scattering occurs at scattering vectors with κ_x between 0 and l and with κ_y between 0 and π/D. Here, l is the minimum of $\pi/(a\cos\theta)$ and $\pi/(E\sin\theta)$. Generally, D and E are large such that, for all θ values except for θ values closely around 0, the scattering occurs at scattering angles smaller than the aperture of the analyzer.

[1]G. M. Drabkin, E. I. Zabidarov, Ya. A. Kasman, and A. I. Okorokov, Zh. Eksp. Teor. Fiz. **56**, 478 (1969) [Sov. Phys. JETP **29**, 261 (1969)].
[2]M. Th. Rekveldt, J. Phys. (Paris) Colloq. **32**, C1-579 (1971).
[3]A. I. Okorokov, V. V. Runov, V. I. Volkov, and A. G. Gukasov, Zh. Eksp. Teor. Fiz. **69**, 590 (1975) [Sov. Phys. JETP **42**, 300 (1975)].
[4]G. M. Drabkin, E. I. Zabidarov, and A. V. Kovalev, Zh. Eksp. Teor. Fiz. **69**, 1804 (1975) [Sov. Phys. JETP **42**, 916 (1975)].
[5]M. Th. Rekveldt, J. Phys. (Paris) Colloq. **38**, C1-23 (1977).
[6]M. Th. Rekveldt, Textures Microstruct. **11**, 129 (1989).
[7]R. Rosman and M. Th. Rekveldt, J. Magn. Magn. Mater. **95**,

319 (1991).
[8]R. Rosman and M. Th. Rekveldt, J. Appl. Phys. (to be published).
[9]R. Rosman and M. Th. Rekveldt, Z. Phys. B **79**, 61 (1990).
[10]R. Rosman, H. Frederikze, and M. Th. Rekveldt, Z. Phys. B **81**, 149 (1990).
[11]C. G. Shull, W. A. Strauser, and E. O. Wollan, Z. Phys. B **83**, 333 (1951).
[12]R. Veitch, BASF, Ludwigshafen, Germany.
[13]Ventron, Beverly, Massachusetts.
[14]L. M. Corliss, J. M. Hastings, and R. J. Weiss, Phys. Rev. Lett. **3**, 211 (1959).
[15]V. N. Bykov, V. S. Golovkin, N. V. Ageev, V. A. Levdik, and S. I. Vinogradov, Dokl. Akad. Nauk SSSR **128**, 1153 (1959) [Sov. Phys. Dokl. **4**, 1070 (1959)].
[16]G. E. Bacon, Acta Crystallogr. **14**, 823 (1961).
[17]G. Shirane and W. J. Takei, J. Phys. Soc. Jpn. Suppl. B3, 35 (1962).
[18]G. E. Bacon, *Neutron Diffraction,* 3rd ed. (Clarendon, Oxford, 1975).
[19]J. Kubler, J. Magn. Magn. Mater. **20**, 277 (1980).
[20]M. O. Steinitz, J. Magn. Magn. Mater. **60**, 137 (1986).
[21]E. Fawcett, Rev. Mod. Phys. **60**, 209 (1988).